Adsorption mechanisms of thallium (I) and thallium (III) by titanate nanotubes: Ion exchange and co-precipitation

Citation for published version:
Borthwick, A, Liu, W, Zhang, P, Chen, H & Ni, J 2014, 'Adsorption mechanisms of thallium (I) and thallium (III) by titanate nanotubes: Ion exchange and co-precipitation', *Journal of Colloid and Interface Science*, vol. 423, pp. 67-75. https://doi.org/10.1016/j.jcis.2014.02.030

Digital Object Identifier (DOI):
10.1016/j.jcis.2014.02.030

Published In:
Journal of Colloid and Interface Science

Accepted Manuscript

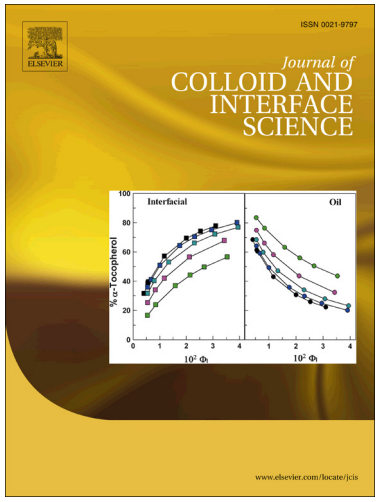

Adsorption mechanisms of thallium(I) and thallium(III) by titanate nanotubes: Ion-exchange and co-precipitation

Wen Liu, Pan Zhang, Alistair G.L. Borthwick, Hao Chen, Jinren Ni

PII: S0021-9797(14)00106-4
DOI: http://dx.doi.org/10.1016/j.jcis.2014.02.030
Reference: YJCIS 19412

To appear in: *Journal of Colloid and Interface Science*

Received Date: 28 December 2013
Accepted Date: 17 February 2014

Please cite this article as: W. Liu, P. Zhang, A.G.L. Borthwick, H. Chen, J. Ni, Adsorption mechanisms of thallium(I) and thallium(III) by titanate nanotubes: Ion-exchange and co-precipitation, *Journal of Colloid and Interface Science* (2014), doi: http://dx.doi.org/10.1016/j.jcis.2014.02.030

Adsorption mechanisms of thallium(I) and thallium(III) by titanate nanotubes: Ion-exchange and co-precipitation

Wen Liu [a, b] Pan Zhang [c] Alistair G.L. Borthwick [d] Hao Chen [c] Jinren Ni [a, b, *]

[a] *Shenzhen Key Laboratory for Heavy Metal Pollution Control and Reutilization, School of Environment and Energy, Peking University Shenzhen Graduate School, Shenzhen 518055, China*

[b] *The Key Laboratory of Water and Sediment Sciences, Ministry of Education, Department of Environment Engineering, Peking University, Beijing 100871, China*

[c] *College of Resources and Environmental Sciences, China Agriculture University, Beijing 100193, China*

[d] *Institute of Energy Systems, School of Engineering, The University of Edinburgh, The King's Buildings, Edinburgh EH9 3JL, U.K.*

*Corresponding author, Tel: (86) 10-6275-1185; Fax: +86-10-62756526

Email: nijinren@iee.pku.edu.cn

Abstract

Hydrothermally-synthesized titanate nanotubes (TNTs) are found to be excellent at adsorption of highly toxic thallium ions. Uptake of both thallium ions is very fast in the first 10 min. The adsorption isotherm of Tl(I) follows the Langmuir model with maximum adsorption capacity of 709.2 mg g^{-1}. Ion-exchange between Tl^+ and Na^+ in the interlayers of TNTs is the primary mechanism for Tl(I) adsorption. Excess Tl^+ undergoes further exchange with H^+. The adsorption mechanism is different for Tl(III), and involves either ion-exchange with Na^+ at low Tl(III) concentration or co-precipitation in the form of $Tl(OH)_3$ with TNTs at high Tl(III) concentration. XPS analysis indicates that the ion-exchange process does not change the basic skeleton [TiO_6] of TNTs, whereas $Tl(OH)_3$ precipitation increases the percentage composition of O within the surface hydroxyl groups. XRD analysis also confirms the formation of $Tl(OH)_3$ on TNTs at high initial concentration of Tl(III). Coexisting Na^+ and Ca^{2+} hardly inhibit adsorption, indicating good selectivity for thallium by TNTs. Furthermore, TNTs can be reused efficiently after HNO_3 desorption and NaOH regeneration, making TNTs a promising material to remove thallium from wastewaters. This study also confirms that co-precipitation is another important adsorption mechanism for easily hydrolytic metals by TNTs.

Keywords: Thallium; Titanate nanotubes; Adsorption; Ion-exchange; Co-precipitation

1. Introduction

Thallium (Tl) is a rare but widespread element in the natural environment, and is found in soils, plants, estuaries and lakes [1-4]. At high concentrations, thallium poses a great threat to the ecosystem and is very damaging to human health. Over the past few decades, thallium and its compounds have been increasingly used in specialized electronic research equipment, semiconductors and lasers, fiber (optical) glass manufacture, scintilla graphic imaging, superconductivity, fireworks, pigments and dyes, and mineralogical separation processes [5-8]. Wastewater emissions, solid waste from coal combustion, metal smelting, and industrial wastewaters are the main anthropogenic sources of thallium.

Tl(I) and Tl(III) are the two main oxidation states of thallium. The chemical properties of Tl(I) are similar to K^+ due to their similar ionic radii, whereas Tl(III) is more like Al^{3+} because it belongs to the IIIA group in the periodic table of elements. Tl(I) can form more stable compounds than Tl(III) which has strong oxidizing properties and is slowly converted to a monovalent state [1, 3]. Consequently, Tl(I) is the most commonly occurring species of thallium in most natural environments [9] .

Thallium is a highly toxic element, and has been called “the element being cursed at birth” [10]. It is more acutely toxic to mammals than more common heavy metals, like Hg, Cd, Pb, Zn, and Cu [11-12]. For example, It was reported that Tl(III) ions are about 34,000 times more toxic than Cd(II) when present in an aquatic environment [13]. Ralph and Twiss [14] reported that Tl(III) is approximately 50,000 times more toxic than Tl(I) to the unicellular chlorophyte, *Chlorella*. When thallium is absorbed through skin and mucous membranes, it becomes widely distributed throughout the body and accumulates in bones, renal medulla and, eventually, in the

central nervous system. Thallium also causes damage to the lungs, heart, liver, and kidneys, and can be fatal [15-17]. The exact mechanism of thallium toxicity is still unclear, so accurate diagnosis of thallium poisoning is difficult to perform and has to be confirmed by chemical analysis [17]. The US Environmental Protection Agency (USEPA) lists thallium as a priority pollutant due to its high toxicity, and proposes specific categories for its treatment and disposal. These are given by the Best Demonstrated Available Technology (BDAT) for the Resource Conservation and Recovery Act (RCRA) thallium wastewater Categories P113, P115, U214, U215, U216, and U217. Treatment technology involves chemical oxidation of Tl(I) compounds followed by chemical precipitation with hydroxide compounds, and then settling and filtration [18]. There is a strict effluent standard for thallium concentration in wastewaters, which must be below 0.14 mg L^{-1}.

Relatively few studies have focused on the removal of thallium from aqueous solutions. The Us Environmental Protection Agency has approved activated alumina precipitation and ion exchange as efficient methods for removing thallium from drinking waters [19]. Alternative methods include precipitation by hydroxides [18], ion-exchange by resin [20], and adsorption by certain materials (such as activated carbon [21], ferrihydrite [22], sawdust [23], biomass [24], and carbon nanotubes [25]). Of these techniques, adsorption is predominantly used because of its high removal efficiency and simplicity in operation. However, for removal of thallium by adsorption, three objectives must be satisfied: efficient removal capability, rapid rate of uptake; and the adsorbent should be easy to re-useable. With these in mind, attention has increasingly focused on the use of titanate nanotubes (TNTs) for treatment of water polluted by heavy metals. TNTs are easily synthesized by a hydrothermal method using TiO_2 and NaOH solution at moderate temperature [26-27].

In addition, TNTs have special physicochemical properties, small tube diameters, large specific surface area, and charged surface. Consequently, TNTs are commonly used as adsorbents for the removal of heavy metal cations such as Cd(II), Pb(II), Cr(III), Cu(II) [28-30], radioactive elements like Cs(I), Sr(II), Ba(II) [31-32], and lanthanides Eu(III) [33-34]. In particular, the adsorption capacity of Pb(II) and Cd(II) onto TNTs can reach 520 and 238 mg g^{-1} respectively, which are much larger values than achieved by most other adsorbents [28]. Besides, TNTs have good sedimentation properties and can easily be re-used [35-36], making them a promising adsorbent for removal of thallium from solution.

This paper examines the adsorption of Tl(I) and Tl(III) on hydrothermally-synthesized TNTs.. Results are presented concerning the adsorption kinetics and isotherms. The effects of pH and coexisting ions on adsorption are investigated. Insight is provided by XPS, XRD and Raman analysis into the different adsorption mechanisms of Tl(I) and Tl(III) on TNTs. Desorption of thallium and regeneration of TNTs are also studied. It is concluded that TNTs have great potential for removal of thallium from aqueous solutions.

2. Materials and methods

2.1 Chemicals and reagents

$Tl(NO_3)_3{\cdot}3H_2O$ and $TlNO_3$ were purchased from Alfa Aesar Company (MA, USA) and dissolved in deionized waters to form Tl(I) and Tl(III) stock solutions (1 L, 1000 mg L^{-1}). 2 mL concentrated nitric acid were added to the Tl(III) solution and the mixture diluted to 1 L in a volumetric flask. $NaNO_3$ and $Ca(NO_3)_2$ were used to form the inorganic stock solution of 1000 mg L^{-1}. All other reagents were of analytical grade or better.

2.2 Preparation of TNTs

TNTs were synthesized via the hydrothermal method [26] [28]. Specifically, 1.2 g of P25 TiO_2 (Degussa, Germany, ca. 90% anatase and 10% rutile) were mixed with 10 mol L^{-1} NaOH solutions. After stirring for 24 h, the mixture was heated at 130 ^{o}C for 72 h in a Teflon container with a stainless steel outer casing. Afterwards, the product was separated by centrifuge (8000 rpm, 5 min) and washed with deionized water until the supernatant pH became neutral. Finally, the precipitate was dried in air at 80 ^{o}C for 4h.

2.3 Adsorption experiments

2.3.1 Batch adsorption experiments

All the batch adsorption experiments were conducted in a rotary shaker (25 ± 0.2 ^{o}C, 200 rpm) using 100 mL Erlenmeyer flasks. The influence of solution pH on adsorption of Tl(I) and Tl(III) by TNTs was studied first. The pH of a 50 mL solution containing 100 mg L^{-1} of thallium ions and 0.2 g L^{-1} of TNTs was adjusted to a target value set between 2 and 6 using diluted HCl and NaOH. After shaking for 180 min, samples were taken and filtered through a 0.22 μm membrane, and then the concentration of thallium measured immediately. For kinetic studies, the initial concentration of thallium ions was altered between 50 and 100 mg L^{-1}, and the solution pH adjusted to 5 for Tl(I) with diluted HCl and 2 for Tl(III) with diluted NaOH. Solutions were shaken for 4 h and samples were taken at specific intervals. For isotherm studies, the initial concentration of thallium ions was varied from 10 to 150 mg L^{-1}. Solution pH was adjusted to 5 for Tl (I) and 2 for Tl(III). After shaking for 3 h, samples were taken and the concentration of thallium measured immediately afterwards. For influence of inorganic ions, concentrations of Tl(I) and Tl(III) were

fixed at 100 mg L^{-1} and the concentrations of coexisting Na^+ and Ca^{2+} varied from 50 to 200 mg L^{-1}, while all other operations were the same as for the previous experiments.

After the supernates were diluted by deionized water, concentrations of thallium ions were determined by means of inductively coupled plasma-mass spectrometry (ICP-MS, X Series II, Thermo Fisher Scientific, USA). The adsorption capacity of thallium on TNTs was calculated from:

$$q_e = \frac{(C_0 - C_e)V}{m} \quad (1)$$

where q_e (mg g^{-1}) is the adsorption capacity at equilibrium, C_0 (mg L^{-1}) and C_e (mg L^{-1}) are the initial and equilibrium concentrations of the thallium ions respectively, V (L) is the total solution volume, and m (g) is the mass of TNTs added in solution.

The removal efficiency (R, %) of thallium ion from aqueous solution was obtained using:

$$R = \frac{(C_0 - C_e)}{C_0} \times 100\% \quad . \quad (2)$$

2.3.2 Measurement of Na content

Once the isotherm experiments had been completed, the Na contents of fresh TNTs and TNTs with Tl(I) adsorbed were measured after microwave digestion. Typically, 15 mg of TNTs were dispersed in 15 mol/L concentrated nitrate acids, and the materials then completely dissolved through microwave digestion. Meanwhile, a blank experiment was also carried out to eliminate the interference of impurities from acids and deionized water. Finally, the solutions were diluted to prescribed volumes, and the Na concentration was measured immediately by ICP-MS.

2.4 Desorption and regeneration experiments

Desorption and regeneration studies were based on the adsorption experiments. Firstly, 0.01 g TNTs were added into the thallium solutions (100 mg L^{-1}) in a 50 mL flask with pH 5 for Tl(I) and pH 2 for Tl(III) respectively, and then shaken for 3 h to reach adsorption equilibrium. Samples were taken and the thallium concentration was determined. A prescribed volume of concentrated nitric acid (ca. 16.4 mol L^{-1}) was added to the solutions in order for the final H^+ concentration to be about 0.2, 0.4 and 0.6 mol L^{-1}, respectively. After stirring for 3 h, the concentration of thallium was determined. The desorption degree (D, %) was calculated form:

$$D = \frac{(C_d - C_e)}{(C_0 - C_e)} \times 100\% \quad (3)$$

where C_d (mg L^{-1}) is the concentration of thallium after desorption.

After desorption, the TNTs were separated and immersed into 0.2 M NaOH solution for 3 h to regenerate the tubular structure [35], and the regenerated TNTs reused to adsorb Tl(I) and Tl(III). The adsorption-desorption-regeneration process lasted for two cycles.

1.5 Characterization methods

The morphology of the TNTs before and after adsorption was analyzed using Tecnai T20 Transmission electron microscopy (TEM) operating at 200 kV, with dedicated software provided by DigitalMicrograph. The energy dispersive X-ray spectrum (EDX) was measured. The crystal phase of the sample was visualized by a X-ray diffractometer (XRD, D/max-2400, Rigaku, Japan) operating at 100 kV and 40 mA and using Cu $K\alpha$ radiation (λ = 1.542 Å), at a scan speed of 4°/min. The element composition and corresponding oxidation state were obtained using X-ray

photoelectron spectroscopy (XPS, AXIS-Ultra, Kratos Analytical, England) at 15 mA and 15 kV with an Al *Kα* X-ray source (225 W), where all binding energies were calibrated with C 1s peak at 284.80 eV to compensate for surface charge effects. Raman spectra were recorded on a RM-1000 (Renishaw, UK) with 514 nm excitation from a He-Ne laser.

3. Results and discussion

3.1 Morphology of TNTs

As shown in Fig.1a, the TNTs comprised multi-layers of hollow, open-ended tubes, each of uniform cross-section with 4.7 nm inner diameter and 9.2 nm outer diameter. As a result, the nanotubes had large specific surface area (272.31 $m^2 g^{-1}$) [26] of great help for metal adsorption. The EDX spectrum indicated that TNTs contained Na, Ti and O, consistent with sodium titanate [37-38]. Sodium titanate is the main component of TNTs, and is written as $Na_xH_{2-x}Ti_3O_7{\cdot}nH_2O$ (x = 0 to 0.75, depending on the remaining sodium ions) [27, 37]. Zigzag ribbons of edge-sharing [TiO_6] octahedrons formed the basic skeleton of the TNTs, before curling up into multilayered tubes. H^+ and Na^+ ions were located in the interlayers, being promoted by the adsorption of cations [30]. After adsorption of Tl(I) (Fig.1b), many nanotubes were broken, giving the surface a coarse texture. After adsorption of Tl(III), precipitates were observed attached to the tubes (Fig.1c). Thallium peaks occur in the EDX spectra after adsorption (Fig.1b and 1c), indicating that both Tl(I) and Tl(III) became attached to the TNTs.

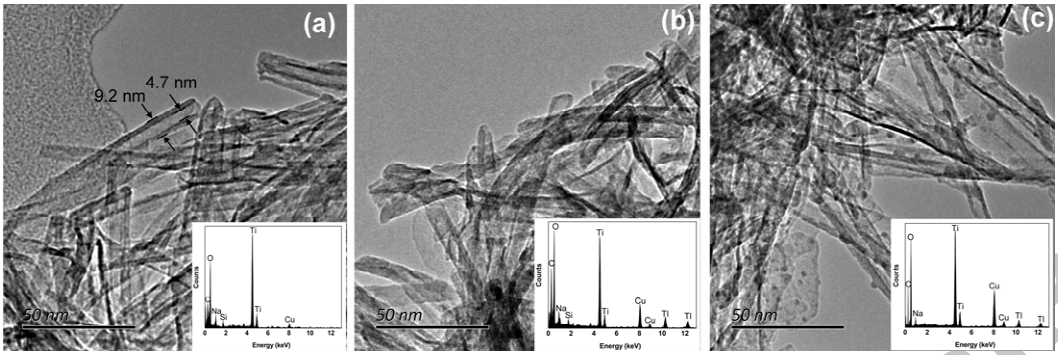

Fig.1. TEM images and EDX spectra of TNTs: (a) before adsorption of thallium; (b) after absorption of thallium Tl(I); and (c) after absorption of thallium Tl(III).

3.2 Adsorption behavior of Tl(I) and Tl(III) on TNTs

3.2.1 Effect of pH

Solution pH affects the surface charge of TNTs and the concentration of metal species in solution [29], and so is an important factor in adsorption. Fig.S1 and Fig.S2 present the zeta potential of TNTs and the thallium species distributions for different pH. The point of zero charge of TNTs is 2.56 (Fig.S1). Moreover, Tl^+ is the principal species for Tl(I) over a wide range of pH values, but Tl(III) hydrolyzes drastically when pH > 2 (Fig.S2). Fig.2 shows the effect of pH on adsorption of Tl(I) and Tl(III) by TNTs. The adsorption capacities of both Tl(I) and Tl(III) rise with increasing pH, but the mechanisms are different. For Tl(I), at low pH of 1–2, the surface charge of the TNTs was positive, and so electrostatic repulsion between Tl^+ and positively-charged TNTs inhibited adsorption, resulting in low uptake of Tl(I) (25.4 mg g^{-1} at pH 1 and 76.2 mg g^{-1} at pH 2). Meanwhile, excess H^+ competed with Tl^+ for active sites at low pH. When the pH increased from 2 to 3, the surface charge of the TNTs turned negative, which benefited the adsorption of Tl^+, corresponding to the rapid rise observed in adsorption capacity from 2 to 3. For further increase in pH, the

amount of negative charge increased and fewer H^+ ions coexisted in solution, leading to enhanced adsorption capacity. Almost 100% removal efficiency was achieved when pH was above 5, indicating the excellent adsorption performance of TNTs.

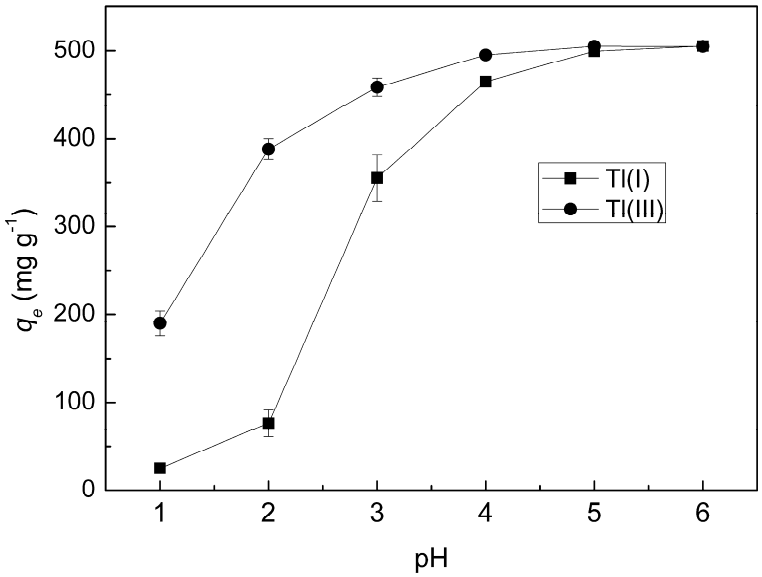

Fig.2. Effect of pH on adsorption of Tl(I) and Tl(III) by TNTs. (TNTs dosage 0.2 g L^{-1}; temperature 25 ^{o}C).

For adsorption of Tl(III), although TNTs were positively charged at pH 1–2, hydrolysis of Tl(III) occurred, as a result of $Tl(OH)_3$ formation. Consequently, Fig.2 shows a larger adsorption capacity of Tl(III) (189.8 mg g^{-1} at pH 1 and 388.3 mg g^{-1} at pH 2) than that of Tl(I). For solution pH > 3, precipitation in the form of $Tl(OH)_3$ was the dominant mechanism for Tl(III) removal. This effect was enhanced at higher pH, leading to enhanced adsorption capacity and high removal efficiency.

3.2.2 Adsorption kinetics

Fig.3 illustrates the adsorption kinetics of Tl(I) and Tl(III). Rapid uptake occurs in the first 30 min (especially the initial 10 min), due to the large amount of active sites on the surface of the TNTs [28, 30]. The adsorption rate of Tl(III) was a little lower than that of Tl(I) during the initial stage, because complicated components including $Tl(OH)^{2+}$, $Tl(OH)_2^+$ and $Tl(OH)_3$ coexisted in solution at the experimental pH (2), resulting in heterogeneous adsorption onto the TNTs. Both of the thallium ions reached equilibrium within 90 min, indicating that 180 min was sufficiently long for the subsequent adsorption experiments.

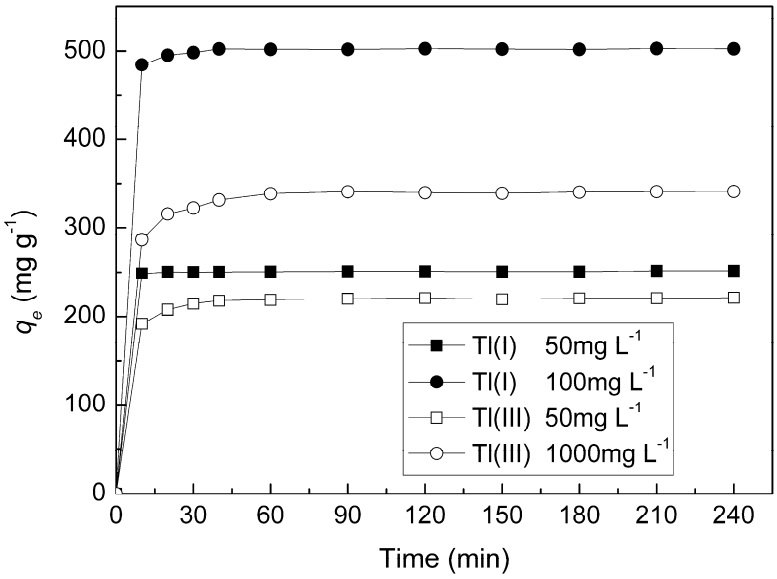

Fig.3. Adsorption kinetics of Tl(I) and Tl(III) on TNTs. (TNTs dosage 0.2 g L^{-1}; temperature 25 ^{o}C; pH 5 for Tl(I) and pH 2 for Tl(III)).

Pseudo-first-order and pseudo-second-order models are used to analyse the adsorption kinetics results, and are expressed as [39-40]:

Pseudo-first-order model: $$q_t = q_e - q_e \exp(-k_1 t) \quad (4)$$

Pseudo-second-order model: $$\frac{t}{q_t} = \frac{1}{k_2 q_e^2} + \frac{t}{q_e} \quad (5)$$

where q_t and q_e (mg g^{-1}) are the adsorption capacities of thallium at time t (min) and equilibrium, respectively. k_1 (min^{-1}) and k_2 (g $mg^{-1}min^{-1}$) are the rate constants of the pseudo-first-order and pseudo-second-order kinetic models, respectively.

Table 1 lists the corresponding kinetic parameters. The kinetic results are closely fitted by the pseudo-second-order model, with a high correlation coefficient ($R^2 \geq 0.9999$). This indicates that the rate-controlling step for adsorption was chemical interaction, exhibited by the initial diffusion of metal ions from solution to TNTs' surface, and the subsequent interaction between –ONa/ –OH groups of TNTs and metal ions [40].

Table 1. Kinetic parameters for adsorption of Tl(I) and Tl(III) on TNTs.

Kinetic model	Parameters	Initial Tl(I) concentration (mg L^{-1})		Initial Tl(III) concentration (mg L^{-1})	
		50	100	50	100
Pseudo-first-order model	q_e (mg g^{-1})	4.35	9.97	24.13	56.89
	k_1 (min^{-1})	0.0151	0.0231	0.0239	0.0295
	R^2	0.2475	0.3772	0.7003	0.7902
Pseudo-first-order model	q_e (mg g^{-1})	251.3	502.5	221.7	342.5
	k_2 (g mg^{-1} min^{-1})	0.0311	0.0172	0.0046	0.0021
	R^2	1.0000	1.0000	1.0000	0.9999

3.2.3 Adsorption isotherms

Two models are introduced to study the adsorption isotherm process of Tl(I) and Tl(III) onto TNTs, namely the Langmuir [41] and the Freundlich [42] models, which can be written as:

Langmuir model: $$q_e = \frac{q_{max} K_L C_e}{1 + q_{max} C_e} \quad (6)$$

Freundlich model: $$q_e = K_F C_e^{1/n} \quad (7)$$

in which q_e (mg g^{-1}) and C_e (mg g^{-1}) are the adsorption capacity and concentration of thallium at equilibrium. q_{max} (mg g^{-1}) represents the maximum adsorption capacity, and K_L (L mg^{-1}) is the Langmuir constant related to the adsorption energy. K_F (mg g^{-1}) is the Freundlich constant related to adsorption capacity and n is the heterogeneity factor indicating the adsorption intensity of the adsorbate.

The adsorption isotherms are shown in Fig.4, and the corresponding parameters are listed in Table 2. The adsorption isotherm of Tl(I) presents a good Langmuir fit ($R^2 > 0.99$), implying that the active sites were distributed homogenously on the TNTs, and that monolayer adsorption occurred. The simulated maximum adsorption capacity of Tl(I) reached 709.2 mg g^{-1}, a considerably larger value than obtained for other common adsorbents like TiO_2 (ca. 4.6 mg g^{-1}) [43], sawdust (ca. 13.2 mg g^{-1}) [23] and powdered leaves (ca. 80.7 mg g^{-1}) [44]. Ion-exchange between Na^+ or H^+ was widely demonstrated to be the main mechanism for the metal cation adsorption onto TNTs [30, 38, 45]. The adsorption process of Tl(I) could therefore be expressed:

$$x\,Tl^+ + (Na, H)_2Ti_3O_7 \rightarrow Tl_x(Na,H)_{2-x}Ti_3O_7 + x\{Na^+, H^+\} \quad (8)$$

in which $(Na, H)_2Ti_3O_7$ represents TNTs, and $\{Na^+, H^+\}$ are the ions exchanged from

287 the TNTs.

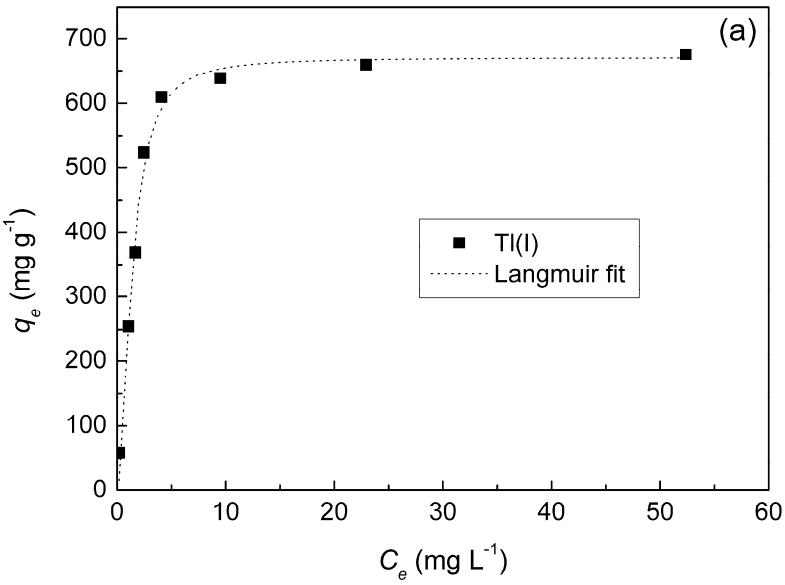

288

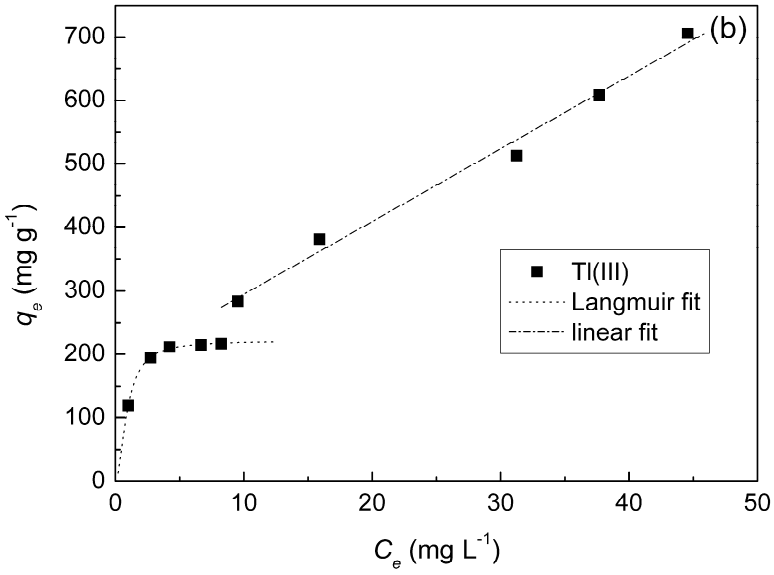

289

290 **Fig.4.** Isotherms for adsorption of (a) Tl(I) and (b) Tl(III) on TNTs. (TNTs dosage 0.2

291 g L^{-1}; temperature 25 ^{o}C, pH 5 for Tl(I) and pH 2 for Tl(III)).

Table 2. Isotherm parameters for adsorption of Tl(I) and Tl(III) on TNTs.

Isotherm Model	Parameters	Tl(I)	Tl(III)	
			Whole stage	First stage
Langmuir model	q_{max} (mg g^{-1})	709.2	847.5	241.0
	K_L (L mg^{-1})	0.72	0.07	1.26
	R^2	0.9956	0.8760	0.9963
Freundlich model	K_F (mg g^{-1})	9.52	107.3	130.0
	n	1.79	2.19	3.55
	R^2	0.8569	0.9461	0.8620

As shown in Fig.4b neither the Langmuir or Freundlich model in isolation could describe properly the adsorption isotherm of Tl(III). Instead, the isotherm of Tl(III) on TNTs has two distinct stages. At low Tl(III) equilibrium concentration (<10 mg L^{-1}), the isotherm exhibited a good Langmuir fit (R^2 > 0.99). During this stage, adsorption was dominated by ion-exchange between Tl(III) ions and Na^+/H^+ of TNTs, which included the following reactions:

$$x\,Tl(OH)^{2+} + (Na, H)_2Ti_3O_7 \rightarrow \{Tl(OH)\}_x(Na,H)_{2-2x}Ti_3O_7 + 2x\{Na^+, H^+\}\,, \quad (9)$$

$$x\,Tl(OH)_2^{+} + (Na, H)_2Ti_3O_7 \rightarrow \{Tl(OH)_2\}_x(Na,H)_{2-x}Ti_3O_7 + x\{Na^+, H^+\}\,. \quad (10)$$

At high Tl(III) equilibrium concentration, the adsorption capacity of Tl(III) increased almost linearly with initial concentration, due to precipitation of Tl(III) onto TNTs. It should be noted that there was co-precipitation of Tl(III) with TNTs during the adsorption process because no precipitates were detected in solutions without addition of adsorbents. Co-precipitation of metals and TNTs was also demonstrated

by the study of Pd(II) adsorption on TNTs [46]. The abundant –OH groups of TNTs played an important role in the co-precipitation process. Following the well-established surface precipitation model [47-48], co-precipitation of Tl(III) on the surface of TNTs may be described by the following reactions:

$$\equiv\text{Ti-OH} + \text{Tl(OH)}^{2+} + \text{H}_2\text{O} \rightarrow \equiv\text{Ti-O-Tl(OH)}_2\text{H}^+ + \text{H}^+ \quad (11)$$

$$\equiv\text{Ti-O-Tl(OH)}_2\text{H}^+ + \text{Tl(OH)}^{2+} + 2\text{H}_2\text{O} \rightarrow \{\equiv\text{Ti-O-Tl(OH)}_2\text{H}^+\cdot\text{Tl(OH)}_3\}(\text{s}) + 2\text{H}^+ \quad (12)$$

$$\equiv\text{Ti-OH} + \text{Tl(OH)}_2^+ + \text{H}_2\text{O} \rightarrow \equiv\text{Ti-O-Tl(OH)}_3\text{ H} + \text{H}^+ \quad (13)$$

$$\equiv\text{Ti-O-Tl(OH)}_3\text{ H} + \text{Tl(OH)}_2^+ + \text{H}_2\text{O} \rightarrow \{\equiv\text{Ti-O-Tl(OH)}_3\text{H}\cdot\text{Tl(OH)}_3\}(\text{s}) + \text{H}^+ \quad (14)$$

3.2.4 Adsorption thermodynamics

The effect of temperature on adsorption is now considered, and the adsorption thermodynamic process discussed. The following thermodynamic parameters, free energy change (ΔG, kJ mol^{-1}), enthalpy change (ΔH, kJ mol^{-1}) and entropy change (ΔS, J mol^{-1} K^{-1}), are defined by [49]:

$$K_c = \frac{C_0 - C_e}{C_e} \quad , \quad (15)$$

$$\Delta G = -RT \ln K_c \quad , \quad (16)$$

and

$$\Delta G = \Delta H - T\Delta S \quad , \quad (17)$$

where Kc is the equilibrium constant for the metal ions, R (J mol^{-1} K^{-1}) is the ideal gas constant, and T (K) is the absolute temperature.

Table 3 lists the thermodynamic parameters. It is evident that the adsorption capacity of Tl(I) and Tl(III) decreased with increasing temperature. The negative values of ΔG indicate that the adsorption process of thallium was naturally spontaneous. Furthermore, the negative ΔH values imply (i) that the adsorption process was exothermic, due to hydrated metal ions in solution dissociating into free ions that are then exchanged with H^+/Na^+ [30], and (ii) that the overcoming of the dehydration energy of thallium ions during adsorption was exothermic [29]. Moreover, adsorption involved metal ions transferring from liquid phase to solid phase, weakening the randomness of the liquid-solid system, hence reducing *S*.

Table 3. Thermodynamic parameters for adsorption of Tl(I) and Tl(III) on TNTs.

Metal ion	Temperature (K)	Adsorption capacity (mg g^{-1})	ΔG (kJ mol^{-1})	ΔH (kJ mol^{-1})	ΔS (J mol^{-1} K^{-1})
Tl(I)	293	483.3	-8.44	-44.20	-21.42
	303	477.0	-8.07		
	313	475.7	-7.56		
Tl(III)	293	370.8	-2.41	-41.03	-14.46
	303	354.6	-2.07		
	313	322.9	-1.59		

3.2.5 Effect of coexisting ions

Fig.5 depicts the effect of coexisting Na^+ and Ca^{2+} ions on adsorption of thallium. The adsorption capacity of Tl(I) on TNTs decreased with increasing inorganic ion

concentration, because the coexisting cations competed for adsorption sites with Tl(I). Bivalent Ca^{2+} had larger affinity with TNTs than Na^{+}, so the inhibition effect was more obvious. However, TNTs still exhibited a large adsorption capacity in the presence of Na^{+} and Ca^{2+}, and the adsorption capacity only decreased 14.5% even when 200 mg L^{-1} Ca^{2+} coexisted. However, the coexisting inorganic ions seemed to have little effect on the adsorption of Tl(III) because the primary mechanism was precipitation for Tl(III), and positively-charged TNTs could hardly capture Na^{+}/Ca^{2+} at pH 2. Therefore, TNTs exhibited high adsorption selectivity for Tl(I) and Tl(III). This is of considerable benefit to the eventual application of TNTs to full-scale wastewater treatment.

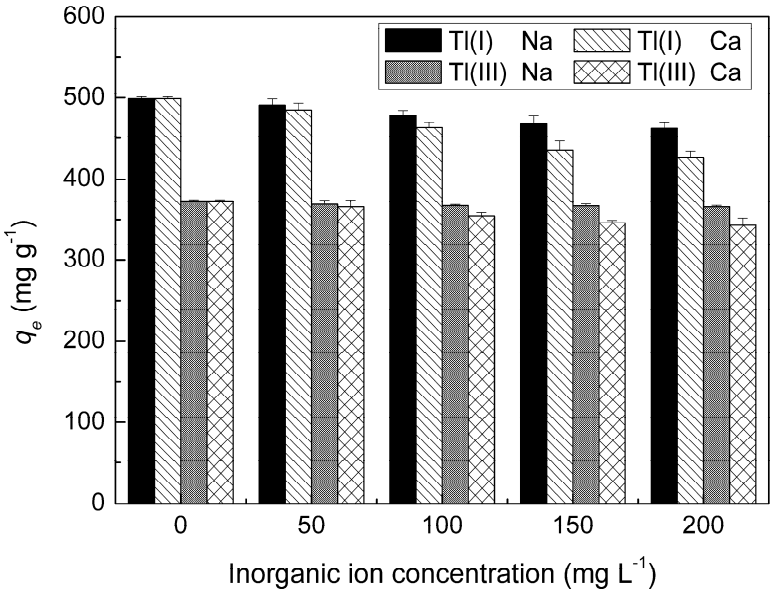

Fig.5. Effect of coexisting ions on adsorption of Tl(I) and Tl(III) by TNTs. (TNTs dosage 0.2 g L^{-1}; temperature 25 ^{o}C; pH 5 for Tl(I) and pH 2 for Tl(III)).

3.2 Adsorption mechanisms of Tl(I) and Tl(III) on TNTs

Adsorption of Tl(I) by TNTs involves a single ion-exchange process between Tl^+ and Na^+/H^+ located in the interlayers; however, there are two stages for Tl(III) adsorption: the ion-exchange dominant stage, and the co-precipitation dominant stage. Table 4 presents the relationship between adsorbed Tl^+ and exchanged Na^+/H^+. The Na content of fresh TNTs was determined to be 3.330 mmol g^{-1}, and so the chemical composition of TNTs could be written as $Na_{0.8}H_{1.2}Ti_3O_7 \cdot 1.8H_2O$, consistent with previous findings [30]. When the initial Tl(I) concentration was low, the Na^+ exchange mechanism completely dominated, its contribution usually exceeding 99% (Table 4). H^+ exchange played a small role in adsorption and in the other mechanisms including surface complexation [50]. As the initial concentration increased (0.964 and 1.010 mg L^{-1}), all the Na^+ ions in TNTs were exchanged by Tl^+, after which excess Tl^+ further exchanged with H^+, resulting in an increasing contribution of H^+ exchange for adsorption (1.09% for 0.964 mg L^{-1} and 2.22% for 1.010 mg L^{-1}). It can therefore be concluded that Na^+ exchange is the dominant mechanism for adsorption of Tl(I). Tl^+ will preferentially exchange with Na^+, and only excess Tl^+ will exchange with H^+.

371 **Table 4.** Contribution of different mechanism on adsorption of Tl(I).

Initial Tl(I) concentration (mol L^{-1})	Capacity (mmol g^{-1})			Contribution (%)		
	total	Na^+ exchange	H^+ exchange [a]	Na^+ exchange	H^+ exchange	Others mechanisms
0.058	0.286	0.284	0.001	99.3	0.35	0.35
0.254	1.246	1.241	0.003	99.6	0.24	0.16
0.525	2.564	2.549	0.010	99.4	0.39	0.19
0.671	3.124	3.107	0.014	99.5	0.45	0.09
0.964	3.376	3.330	0.037	98.6	1.09	0.27
1.010	3.418	3.330	0.076	97.4	2.22	0.35

372 [a] Amount of exchanged H^+ was calculated by precise measurement of pH value before and after adsorption.

For adsorption of Tl(III), although ion-exchange was the main mechanism when the initial ion concentration was low, the species of Tl(III) were complicated and other mechanisms also existed. The numerical relationship between adsorbed Tl(III) and exchange Na^+/H^+ was uncertain, and as a result, various characterization methods including XPS, XRD and Raman spectrum analysis were used to provide insight into the interaction of thallium ions with TNTs.

TNTs after adsorption of Tl(I), Tl(III) at low and high initial concentration are marked as TNTs-Tl(I), TNTs-Tl(III) and TNTs-$Tl(OH)_3$, respectively. Fig.6a presents the XPS survey spectra, where it can be seen that the Na 1s peak weakens considerably after adsorption of either Tl(I) or Tl(III) whereas Tl 4f peaks appear, indicating that ion-exchange took place between Na^+ and thallium ions in the adsorption process. For high resolution of O 1s, the peak at 532.5 eV and 530.1 eV is assigned to O from the surface hydroxyl group (Ti-OH) and $[Ti\text{-}O]_6$ octahedrons (Fig.6b) [51]. Consistent with results from previous studies [29-30], the ion-exchange process did not alter the chemical composition of O, noting that the percentage of O from Ti-OH only changed form 5.6% for TNTs to 6.4% for TNTs-Tl(I) and 8.4% for TNTs-Tl(III). Therefore, ion-exchange took place solely in the interlayers of TNTs, and did not change the basic skeleton $[TiO_6]$. The situation was different for TNTs-$(OH)_3$ where the chemical percentage of O from Ti-OH increased to 13.3% because $Tl(OH)_3$ precipitated on the surface of TNTs.

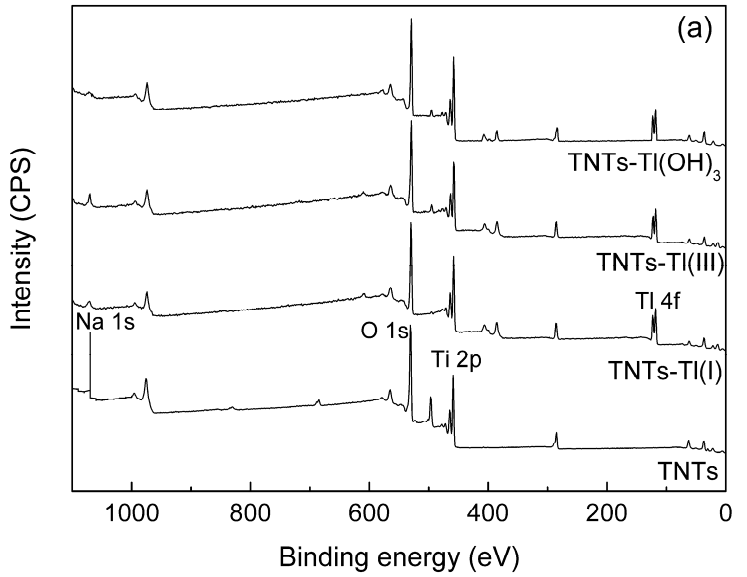

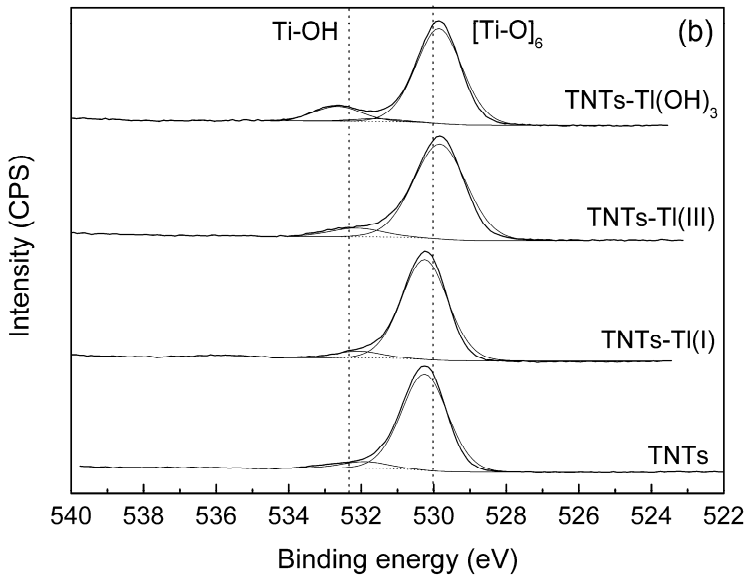

Fig.6. XPS spectra for TNTs before and after adsorption of thallium: (a) survey; and (b) high resolution plot in vicinity of O 1s.

In the XRD patterns (Fig.7), the peaks at ~24°, 28°, 48° and 62° all relate to diffractions of sodium titanate [37, 52]. The intense peak at about 10° represents the interlayer space of TNTs. After adsorption of Tl(III), new peaks corresponding to Tl_2O_3 (avicennite) are evident [53], resulting from $Tl(OH)_3$ decomposition in air. By comparison, diffraction of Tl_2O_3 phase in the pattern of TNTs-$Tl(OH)_3$ is more obvious than that for TNTs-Tl(III), indicating Tl(III) precipitation predominantly occurred when the initial Tl(III) concentration was high. Moreover, the intensity of interlayer diffraction (10°) greatly reduced after adsorption, implying that adsorption of Tl(I) and Tl(III) had broken the interlayer structure of TNTs. Previous studies also report that adsorption of metal ions introduced slight disorder to the layered structure of TNTs and weakened the diffraction at 10° [54]. Adsorption of thallium onto TNTs was an exothermic process, causing damage to the interlayer structure of the TNTs. Besides, $Tl(OH)_3$ precipitates were also blocked in the interlayers (Fig.1c), so that TNTs-$Tl(OH)_3$ exhibited weaker diffraction at 10° that TNTs-Tl(III).

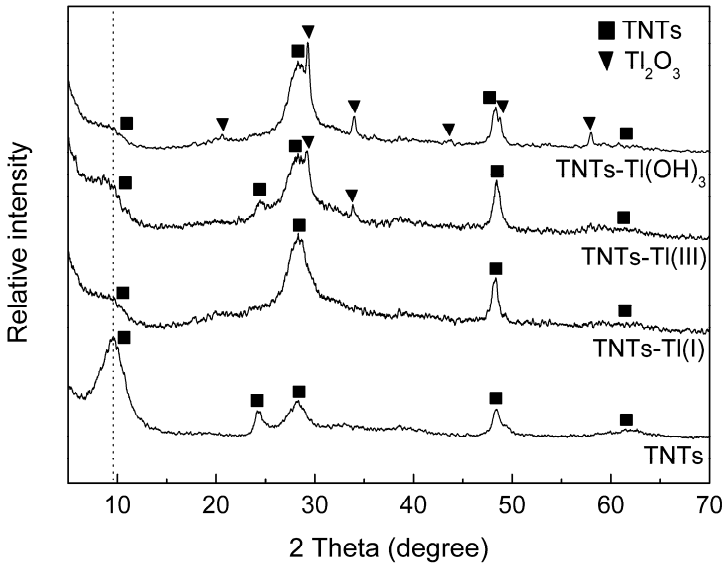

Fig.7. XRD patterns of TNTs before and after adsorption of thallium.

Fig.8 shows the Raman spectra of TNTs before and after adsorption of thallium. For fresh TNTs, the spectra were the same as for tri-titanate prepared under low NaOH concentration or low temperature [38, 55]. The peak at 444 cm^{-1} is ascribed to Ti-O bending and stretching vibrations involving six-coordinated titanium and three-coordinated oxygen atoms in the [TiO_6] octahedron. This peak hardly changed after the ion-exchange between thallium ions and Na^+ (for TNTs-Tl(I) and TNTs-Tl(III)), indicating the stability of [TiO_6] skeleton during the adsorption process. The peak at 905 cm^{-1} is attributed to the short Ti–O stretching vibration related to Na^+, namely, Ti-O-Na. After adsorption of Tl(I), the peak shifted to lower frequencies due to ion-exchange between Tl^+ and Na^+, consistent with previous research findings [38]. A peak at 818 cm^{-1} corresponding to Ti-O-Tl appears, effectively replacing the original Ti-O-Na peak. After adsorption of Tl(III) at low initial concentration, although the Ti-O-Tl peak emerges at 820 cm^{-1}, the Ti-O-Na peak weakens because of incomplete ion-exchange involving Tl^{3+} and Na^+. The situation is quite different for TNTs-$Tl(OH)_3$, where weak peaks of Ti-O-Tl and Ti-O-Na can be observed, and the peak at 444 cm^{-1} shifts due to the precipitation of $Tl(OH)_3$.

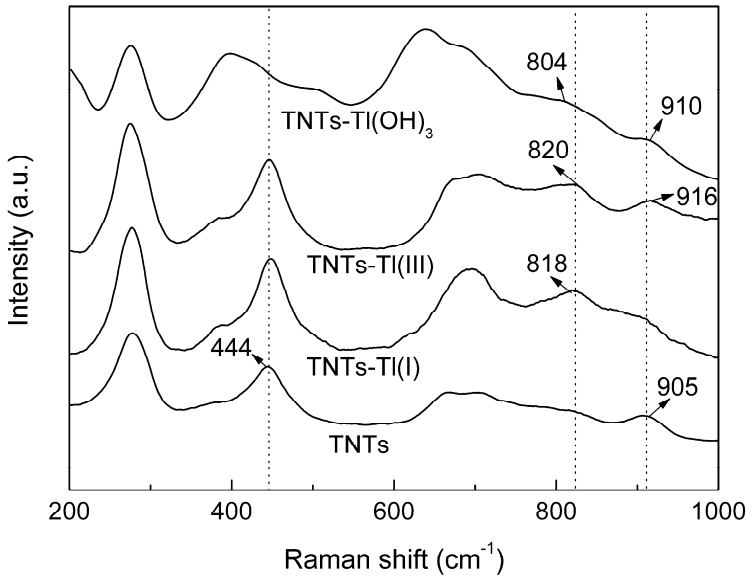

Fig.8. Raman spectra of TNTs before and after adsorption of thallium.

A Schematic diagram of ion-exchange and co-precipitation processes for thallium adsorption onto TNTs is shown in Fig.9. In special, TNTs are full of –ONa and –OH groups on the surface, which are the main adsorption sites for metals. For adsorption of Tl(I), a preferential Na^+ exchange proceeds and a subsequent H^+ exchange occurs (Fig.9a). For adsorption of Tl(III), ion-exchange between Tl(III) ions ($Tl(OH)_2^+$ and $Tl(OH)^{2+}$) and Na^+ happens at low initial Tl(III) concentration (Fig.9b). However, co-precipitation of $Tl(OH)_3$ and TNTs is the primary mechanism at high initial concentration (Fig.9c).

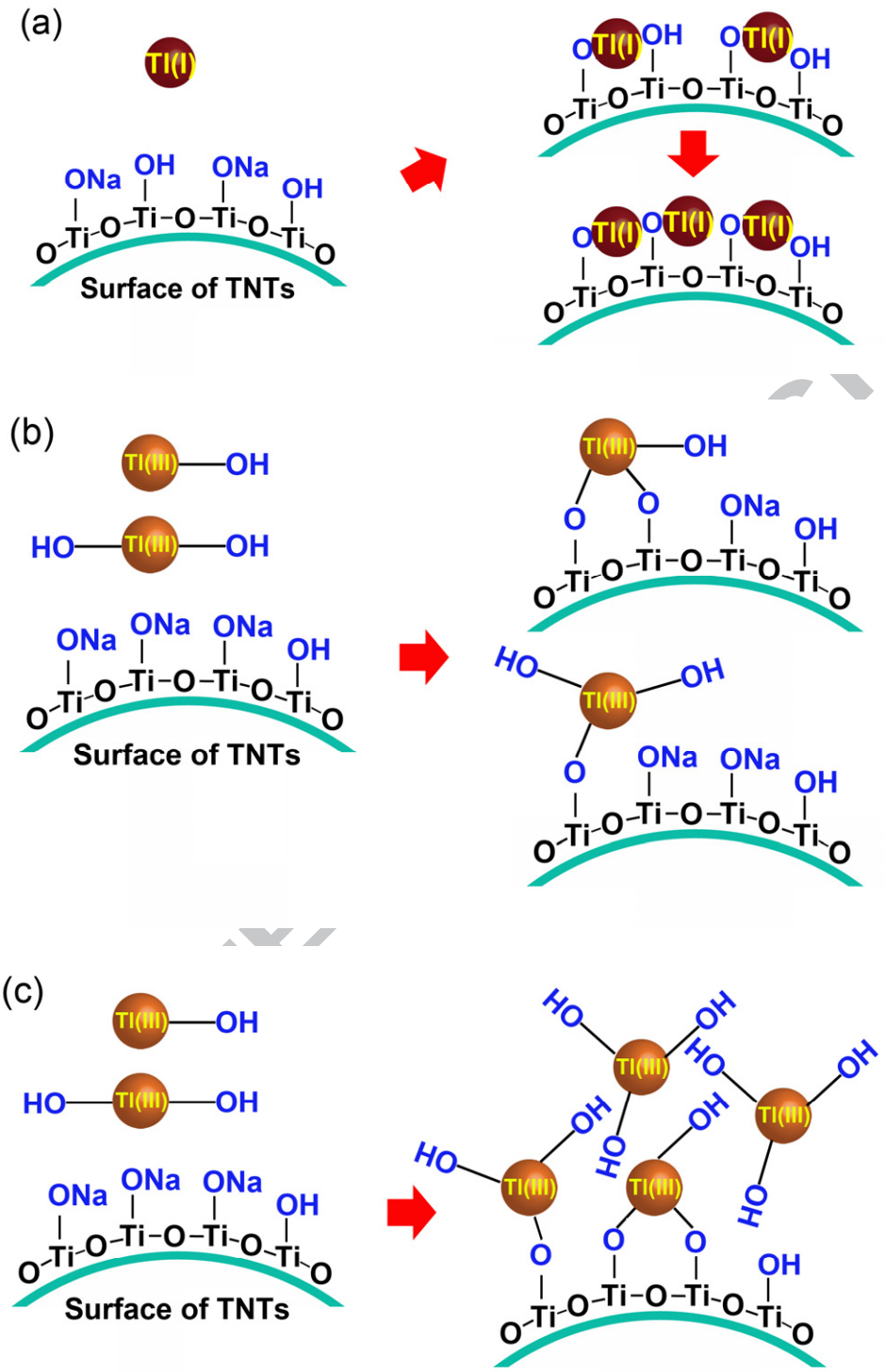

Fig.9. Schematic diagram of (a) Tl(I) and (b), (c) Tl(III) adsorption onto TNTs.

3.4 Reuse of TNTs

TNTs are demonstrably effective adsorbents for metal ions because they have excellent adsorption performance characteristics and can be regenerated easily [35]. Table 5 lists the desorption and regeneration efficiencies of thallium, where it may be seen that Tl(I) was readily desorbed from TNTs by HNO_3, given that the desorption efficiencies were always over 95%. Under HNO_3 treatment, excess H^+ replaced adsorbed Tl^+ on the surface of TNTs [30, 35]. After regeneration by NaOH, the –ONa groups were restored and the adsorption capacity of Tl(I) on regenerated TNTs was little different to that on original TNTs. However, the ratio of adsorption capacity after regeneration to initial capacity q_r/q_0 decreased to 87.7 % when TNTs were desorbed with 0.6 mol L^{-1} HNO_3 and regenerated after two cycles, owing to irreversible damage of TNTs structure under high H^+ concentration. At very high concentration of HNO_3, the tubular structure of TNTs is seriously damaged by H^+, and even phase transition from titanate to anatase can occur [56]. As a result, TNTs could not be fully recovered after NaOH treatment, causing the adsorption capacity to decrease. Desorption of Tl(III) from TNTs was different. $Tl(OH)_3$ precipitation on TNTs was the main adsorption mechanism when the initial Tl(III) concentration was 100 mg L^{-1}. Dissolution of the precipitates was the primary desorption mechanism. Moreover, hydrolysis and –OH complexation of Tl(III) was widespread when the solution H^+ concentration was low, thus reducing the desorption efficiency at low HNO_3 concentration (0.2 mol L^{-1}). However, damage to the TNTs structure occurred when HNO_3 was too high (0.6 mol L^{-1}), so it is concluded that 0.4 mol L^{-1} HNO_3 was a sensible choice for Tl(III) desorption from TNTs.

Table 5. Desorption and regeneration efficiencies of thallium after HNO_3 treatment at different concentrations.

Metal ion	0.2 mol L^{-1} [a]		0.4 mol L^{-1}		0.6 mol L^{-1}	
	Desorption efficiency (%)	q_r/q_0 [a] (%)	Desorption efficiency (%)	q_r/q_0 (%)	Desorption efficiency (%)	q_r/q_0 (%)
Tl(I)	96.4	98.7	98.4	95.3	98.8	90.6
	97.3	97.3	99.0	94.1	99.5	87.7
Tl(III)	72.5	67.1	90.6	91.2	97.7	85.1
	70.7	58.7	92.6	90.5	99.0	80.4

[a] HNO_3 concentration.

[b] Ratio of adsorption capacity after regeneration to initial capacity.

3.5 Environmental implications

As shown above, TNTs can quickly and efficiently remove Tl(I) and Tl(III) from aqueous solutions. Even under extreme conditions such as a solution with low pH, TNTs exhibit a considerable capacity to adsorb thallium ions, especially those of highly toxic Tl(III). TNTs present high adsorption selectivity for thallium ions in the presence of common inorganic ions, and so can be very beneficial in practical wastewater treatment. Furthermore, TNTs can either be reused after moderate treatment, or else be used to trap permanently toxic metals in order to prevent secondary pollution. In short, TNTs can be used as an excellent adsorbent for capturing thallium from aqueous environments, and inhibiting migration of this highly toxic heavy metal to human beings and other living organisms.

4. Conclusion

Hydrothermally-synthesized titanate nanotubes have a layered structure composed of small diameter tubes of large surface area, which can efficiently remove Tl(I) and Tl(III) from aqueous solutions. Laboratory tests reported herein show that the adsorption capacities of Tl(I) and Tl(III) increased with increasing pH. The optimum pH for Tl(I) adsorption was approximately 5–6, whereas efficient adsorption of Tl(III) was found to occur even at a pH as low as 2. The adsorption kinetics of the two metal ions was very rapid, with high removal efficiencies of over 90% observed in the first 10 min of operation. The adsorption isotherm of Tl(I) on TNTs fitted closely to the Langmuir isotherm with a calculated maximum adsorption capacity of 709.2 mg g^{-1}. The adsorption isotherm of Tl(III) comprised two stages: an ion-exchange dominant stage, and a co-precipitation dominant stage. Coexisting Na^{+} and Ca^{2+} slightly decreased the adsorption capacity of Tl(I) and Tl(III), indicating that

TNTs have good adsorption selectivity for both ions. Adsorption of thallium was exothermal, and damaged the layered structure of TNTs.

Ion-exchange between Tl^+ and interlayered Na^+ of TNTs was demonstrated to be the primary mechanism for Tl(I) adsorption. However, the adsorption mechanism was more complicated for Tl(III). At low initial Tl(III) concentration, ion-exchange involving various Tl(III) ions played the pivotal role. At high initial Tl(III) concentration, co-precipitation of $Tl(OH)_3$ and TNTs was the main mechanism for Tl(III) removal, which was further confirmed by XPS and XRD analyses. Besides, XPS showed that the ion-exchange process occurred solely in the interlayers of TNTs, but did not change the basic skeleton of $[TiO_6]$. Co-precipitation is another important adsorption mechanism for easily hydrolytic metal ions, like Pd(II), Ga(III), V(III) and so on.

Finally, TNTs also exhibited a large adsorption capacity for thallium after desorption by HNO_3 and regeneration by NaOH. Titanate nanotubes are excellent adsorbents for removing thallium from wastewaters, and thus have great potential for full-scale treatment processes.

Acknowledgements

Financial support is from the Major Science and Technology Program for Water Pollution Control and Treatment (2010ZX07212-008), Ministry of Science and Technology, China.

Appendix A. Supplementary data

Supplementary data associated with this article are available with the online version.

Reference

[1] T.A. DelValls, V. Saenz, A.M. Arias, J. Blasco, Cienc. Mar. 25 (1999) 161.

[2] A. Tremel, M. Mench, Agronomie. 17 (1997) 195.

[3] T.S. Lin, J. Nriagu, Environ. Sci. Technol. 33 (1999) 3394.

[4] T. Xiao, F. Yang, S. Li, B. Zheng, Z. Ning, Sci. Total. Environ. 421 (2012) 51.

[5] J.O. Nriagu, Wiley Series in Advances in Environmental Science and Technology. John Wiley and Sons, New York,1998.

[6] Z. Assefa, F. Destefano, M.A. Garepapaghi, J.H. Lacasce, S. Ouellete, M.R. Corson, J.K. Nagle, H.H. Patterson, Inorg. Chem. 30 (1991) 2868.

[7] G. Kazantzis, Environ. Geochem. Hlth. 22 (2000) 275.

[8] U. Ewers, Sci. Total. Environ. 71 (1988) 285.

[9] B.W. Vink, Chem. Geol. 109 (1993) 119.

[10] J. Emsley, New Sci. 79 (1978) 392.

[11] V. Cheam, G. Garbai, J. Lechner, J. Rajkumar, Water Qual. Res. J. Can. 35 (2000) 581.

[12] C.H. Lan, T.S. Lin, Ecotox. Environ. Safe. 61 (2005) 432.

[13] B.S. Twining, M.R. Twiss, N.S. Fisher, Environ. Sci. Technol. 37 (2003) 2720.

[14] L. Ralph, M.R. Twiss, Environ. Contam. Tox. 68 (2002) 261-268.

[15] J.J. Rodriguez-Mercado, M.A. Altamirano-Lozano, Drug Chem. Toxicol. 36 (2013) 369.

[16] S. Galvan-Arzate, A. Santamaria, Toxicol. Lett. 99 (1998) 1.

[17] A.L.J. Peter, T. Viraraghavan, Environ. Int. 31 (2005) 493.

[18] R.M.C.L Rosengrant, Final Best Demonstrated 596 Available Technology (BDAT) background document for P and U Thallium wastes. U.S. EPA. Office of Solid waste, Washington, DC. EPA/530-sw-90-059R, National Technical Information Services PB90-234188l; 1990.

[19] U.S.E.E.P. Agency, Technical Factsheet on: Thallium, 2002. <http://www.epa.gov/safewater/dwh/t-ioc/thallium.html>.

[20] R.A. Horne, J. Inorg. Nucl. Chem. 6 (1958) 338.

[21] A. Arifi, H.A. Hanafi, Asian J. Chem. 23 (2011) 111.

[22] T.S. Lin, J.O. Nriagu, Advances in Environmental Science and Technology, Wiley and Sons, New York, (1998) 31.

[23] S.Q. Memon, N. Memon, A.R. Solangi, J.R. Memon, Chem. Eng. J. 140 (2008) 235.

[24] A.L. John Peter, T. Viraraghavan, Bioresource Technol. 99 (2008) 618.

[25] S.U. Rehman, N. Ullah, A.R. Kamali, K. Ali, C. Yerlikaya, H.U. Rehman, New Carbon Mater. 27 (2012) 409.

[26] Q. Chen, W.Z. Zhou, G.H. Du, L.M. Peng, Adv. Mater. 14 (2002) 1208.

[27] Q. Chen, L.M. Peng, Int. J. Nanotechnol. 4 (2007) 44.

[28] L. Xiong, C. Chen, Q. Chen, J.R. Ni, J. Hazard. Mater. 189 (2011) 741.

[29]Y.B. Pu, X.F. Yang, H. Zheng, D.S. Wang, Y. Su, J. He, Chem. Eng. J. 219 (2013) 403.

[30] W. Liu, T. Wang, A.G.L. Borthwick, Y. Wang, X. Yin, X. Li, J. Ni, Sci. Total. Environ. 456 (2013) 171.

[31] D.J. Yang, Z.F. Zheng, H.W. Liu, H.Y. Zhu, X.B. Ke, Y. Xu, D. Wu, Y. Sun, J. Phys. Chem. C 112 (2008) 16275.

[32] D.J. Yang, S. Sarina, H.Y. Zhu, H.W. Liu, Z.F. Zheng, M.X. Xie, S.V. Smith, S. Komarneni, Angew. Chem. Int. Edit. 50 (2011) 10594.

[33] G.D. Sheng, H.P. Dong, R.P. Shen, Y.M. Li, Chem. Eng. J. 217 (2013) 486.

[34] G.D. Sheng, S.T. Yang, D.L. Zhao, J. Sheng, X.K. Wang, Sci. China Chem. 55 (2012) 182.

[35] T. Wang, W. Liu, N. Xu, J. Ni, J. Hazard. Mater. 250 (2013) 379.

[36] W. Liu, W. Sun, A.G.L. Borthwick, J. Ni, Colloids Surf. A 434 (2013) 319.

[37] X.M. Sun, Y.D. Li, Chem. Eur. J. 9 (2003) 2229.

[38] N. Li, L.D. Zhang, Y.Z. Chen, M. Fang, J.X. Zhang, H.M. Wang, Adv. Funct. Mater. 22 (2012) 835.

[39] Y.S. Ho, G. McKay, Chem. Eng. J. 70 (1998) 115.

[40] Y.S. Ho, G. McKay, Process Biochem. 34 (1999) 451.

[41] I. Langmuir, J. Am. Chem. Soc. 40 (1918) 1361.

[42] H. Freundlich, Z. Phys. Chem. 57 (1906) 355.

[43] P. Kajitvichyanukul, C.R. Chenthamarakshan, K. Rajeshwar, S.R. Qasim, Adsorpt. Sci. Technol. 21 (2003) 217.

[44] H.D. Khavidaki, H. Aghaie, Clean Soil Air Water 41 (2013) 673.

[45] N.A. Li, L.D. Zhang, Y.Z. Chen, Y. Tian, H.M. Wang, J. Hazard. Mater. 189 (2011) 265.

[46] H. Kochkar, A. Turki, L. Bergaoui, G. Berhault, A. Ghorbel, J. Colloid Interface

Sci. 331 (2009) 27.

[47] K.J. Farley, D.A. Dzombak, F.M.M. Morel, J. Colloid Interface Sci. 106 (1985) 226.

[48] H.B. Bradl, J. Colloid Interface Sci. 277 (2004) 1.

[49] T. Shi, Z. Wang, Y. Liu, S. Jia, D. Changming, J. Hazard. Mater. 161 (2009) 900.

[50] A.J. Du, D.D. Sun, J.O. Leckie, J. Hazard. Mater. 187 (2011) 401.

[51] H.H. Ou, C.H. Liao, Y.H. Liou, J.H. Hong, S.L. Lo, Environ. Sci. Technol. 42 (2008) 4507.

[52] L. Xiong, Y. Yang, J.X. Mai, W.L. Sun, C.Y. Zhang, D.P. Wei, Q. Chen, J.R. Ni, Chem. Eng. J. 156 (2010) 313.

[53] M. Mohammadi, A. Morsali, Mater. Lett. 63 (2009) 2349.

[54]S.S. Liu, C.K. Lee, H.C. Chen, C.C. Wang, L.C. Juang, Chem. Eng. J. 147 (2009) 188.

[55]R.Z. Ma, K. Fukuda, T. Sasaki, M. Osada, Y. Bando, J. Phys. Chem. B 109 (2005) 6210.

[56] D.V. Bavykin, J.M. Friedrich, A.A. Lapkin, F.C. Walsh, Chem. Mater. 18 (2006) 1124.

Figure Captions

Fig.1. TEM images and EDX spectra of TNTs: (a) before adsorption of thallium; (b) after absorption of thallium Tl(I); and (c) after absorption of thallium Tl(III).

Fig.2. Effect of pH on adsorption of Tl(I) and Tl(III) by TNTs. (Initial metal ion concentration 100 mg L^{-1}; TNTs dosage 0.2 g L^{-1}; temperature 25 ^{o}C).

Fig.3. Adsorption kinetics of Tl(I) and Tl(III) on TNTs. (Initial metal ion concentrations 50 and 100 mg L^{-1} respectively; TNTs dosage 0.2 g L^{-1}; temperature 25 ^{o}C; pH 5 for Tl(I) and pH 2 for Tl(III)).

Fig.4. Isotherms for adsorption of (a) Tl(I) and (b) Tl(III) on TNTs. (TNTs dosage 0.2 g L^{-1}; temperature 25 ^{o}C, pH 5 for Tl(I) and pH 2 for Tl(III)).

Fig.5. Effect of coexisting ions on adsorption of Tl(I) and Tl(III) by TNTs. (Initial thallium ion concentration 100 mg L^{-1}; TNTs dosage 0.2 g L^{-1}; temperature 25 ^{o}C; pH 5 for Tl(I) and pH 2 for Tl(III)).

Fig.6. XPS spectra for TNTs before and after adsorption of thallium: (a) survey; and (b) high resolution plot in vicinity of O 1s.

Fig.7. XRD patterns of TNTs before and after adsorption of thallium.

Fig.8. Raman spectra of TNTs before and after adsorption of thallium.

Fig.9. Schematic diagram of (a) Tl(I) and (b), (c) Tl(III) adsorption onto TNTs.

Table Legends

Table 1. Kinetic parameters for adsorption of Tl(I) and Tl(III) on TNTs.

Table 2. Isotherm parameters for adsorption of Tl(I) and Tl(III) on TNTs.

Table 3. Thermodynamic parameters for adsorption of Tl(I) and Tl(III) on TNTs.

Table 4. Contribution of different mechanism on adsorption of Tl(I).

Table 5. Desorption and regeneration efficiencies of thallium after HNO_3 treatment at different concentrations.

Graphical abstract

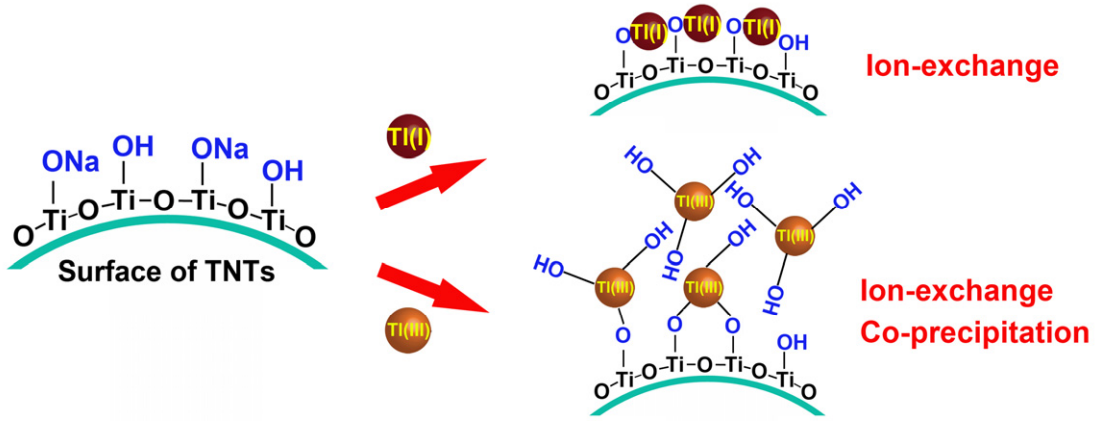

Highlights

- ✓ TNTs show large adsorption capacities for both Tl(I) and Tl(III)
- ✓ Ion-exchange between Tl^+ and Na^+ is the primary mechanism for Tl(I) adsorption
- ✓ Ion-exchange plays the main role in adsorption at low Tl(III) concentration
- ✓ Co-precipitation of $Tl(OH)_3$ and TNTs is dominant at high Tl(III) concentration
- ✓ TNTs can be re-used efficiently after HNO_3 desorption and NaOH regeneration